Analytica Chimica Acta 1184 (2021) 339023

Contents lists available at ScienceDirect

Analytica Chimica Acta

journal homepage: www.elsevier.com/locate/aca

In-depth triacylglycerol profiling using MS^3 Q-Trap mass spectrometry

Matias Cabruja [a], Josefina Priotti [b], Pablo Domizi [c], Katharina Papsdorf [a], Deanna L. Kroetz [b], Anne Brunet [a], Kévin Contrepois [a, *], Michael P. Snyder [a, **]

[a] Department of Genetics, Stanford University, Stanford, CA, USA
[b] Department of Bioengineering and Therapeutic Sciences, University of California San Francisco, San Francisco, CA, USA
[c] Department of Pediatrics, Stanford University, Stanford, CA, USA

HIGHLIGHTS

- MS method combining MRM and MS^3 for the comprehensive profiling of triacylglycerols.
- Advantages of shotgun targeted methods with the structural information of untargeted LC-MS methods.
- Ready to use and efficient in analyzing triacylglycerols in different matrixes.

GRAPHICAL ABSTRACT

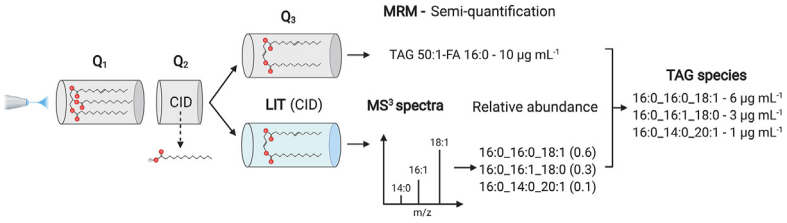

ARTICLE INFO

Article history:
Received 14 June 2021
Received in revised form
7 August 2021
Accepted 30 August 2021
Available online 3 September 2021

Keywords:
Lipids
Triacylglycerols
Fatty acid
Mass spectrometry

ABSTRACT

Total triacylglycerol (TAG) level is a key clinical marker of metabolic and cardiovascular diseases. However, the roles of individual TAGs have not been thoroughly explored in part due to their extreme structural complexity. We present a targeted mass spectrometry-based method combining multiple reaction monitoring (MRM) and multiple stage mass spectrometry (MS^3) for the comprehensive qualitative and semiquantitative profiling of TAGs. This method referred as TriP-MS3 – triacylglycerol profiling using MS^3 – screens for more than 6,700 TAG species in a fully automated fashion. TriP-MS3 demonstrated excellent reproducibility (median interday CV ~ 0.15) and linearity (median $R^2 = 0.978$) and detected 285 individual TAG species in human plasma. The semiquantitative accuracy of the method was validated by comparison with a state-of-the-art reverse phase liquid chromatography (RPLC)-MS ($R^2 = 0.83$), which is the most commonly used approach for TAGs profiling. Finally, we demonstrate the utility and the versatility of the method by characterizing the effects of a fatty acid desaturase inhibitor on TAG profiles *in vitro* and by profiling TAGs in *Caenorhabditis elegans*.

1. Introduction

Triacylglycerols (TAGs) are glycerolipids composed of three fatty acids (FAs) esterified to a glycerol backbone and are specialized in the storage and transport of FAs. The hydrolytic cleavage of TAGs by lipolytic enzymes releases FAs, which are i) the main source of energy production via β-oxidation, ii) precursors for lipid and membrane synthesis, and iii) mediators in cell signaling processes

Abbreviations: TAG, Triacylglycerols: FA; Fatty acids: MRM, Multiple reaction monitoring: MS; Mass spectrometry: LC, Liquid chromatography: MS^2: Tandem mass spectrometry: MS^3: Multiple stage mass spectrometry: IS; Internal standard: CV, Coefficient of variation: R^2: Coefficient of determination.

* Corresponding author.
** Corresponding author.
E-mail addresses: kcontrep@stanford.edu (K. Contrepois), mpsnyder@stanford.edu (M.P. Snyder).

https://doi.org/10.1016/j.aca.2021.339023

[1,2]. Most cells have the capacity to synthesize and store TAGs, but adipose tissue, liver and intestine are the most adept, while skeletal muscle and heart also accumulate TAGs during fasting or exercise [3]. Intracellular TAGs are stored in organelles called lipid droplets and in plasma they are transported in different lipoprotein-containing vesicles (chylomicrons, very-low density lipoproteins, low density lipoproteins). Excess of total TAG content in blood have been associated with a wide array of metabolic diseases including diabetes, cardiovascular and neurodegenerative disease [4] [−] [7]. While this association has long been recognized, the role of individual TAG species has been understudied largely because of technical challenges. Some recent reports showed that not all TAGs behave similarly in diabetes and cardiovascular diseases, hence individual TAG molecules may carry important diagnostic, prognostic or mechanistic information [8]. In addition, a recent multi-omics study revealed two distinct sub-populations of TAGs responding differently to acute aerobic exercise depending on their FA composition [9].

Mass spectrometry (MS) is the technology of choice to analyze complex lipids due to its high sensitivity, specificity and resolution [10]. Extensive TAG cataloguing has been challenging due to their high complexity and similarity [11]. The combination of three different FAs gives rise to thousands of possible TAG molecules, many of which have the same nominal mass, without even considering *sn*-positional isomers, double-bond positions and cis/trans configurations. For instance, up to 43 TAGs with the same mass (878.8 ± 0.1 Da, $[M + NH4]^+$) can be generated with common even and odd chain esterified FAs ranging from 10 to 22 carbons [12]. Furthermore, 18 TAG species were identified in a murine macrophage line (RAW 264.7) with 49 carbons and 2 unsaturations, demonstrating the level of complexity of these lipids in biological samples [12].

TAG profiling is typically performed by liquid chromatography MS (LC-MS) [13] [−] [17]. These methods rely on high resolution mass spectrometers, tandem MS (MS^2) and high chromatographic resolution using reverse phase LC columns (*e.g.* C18, C30). LC-MS approaches are typically untargeted meaning that any TAG above an abundance threshold will be detected. These approaches rely on the chromatographic resolution of TAG isobars and suffer from run-to-run variation which impairs data quality especially in large-scale studies. In addition, processing software must be finely tuned to enable confident automated lipid identification with minimal misidentification rate [8].

On the other hand, targeted lipidomics methods are typically higher throughput, achieve robust quantification and data processing is fast and straightforward. However, limited structural information is obtained in MS^2, identifying only one FA contained in the molecule [18]. Most of these approaches use multiple reaction monitoring (MRM), which consists of filtering ions before and after fragmentation based on *m/z* values. Each pair of *m/z* values are known as a "transition" and in the context of TAG analysis they correspond to the parent TAG molecule and the TAG molecule without one of its FA. Complete TAG characterization can be achieved using multiple stage MS (MS^3) where the ions filtered after MS^2 fragmentation are further fragmented and all the product ions detected. These methods use quadrupole ion-trap or linear ion-trap MS and have been applied to the qualitative characterization of a small number of TAGs [12,19]. Such approach was never employed as a comprehensive screening tool.

In this work, we describe a fully automated shotgun MS strategy using MRM combined with MS^3 to comprehensively profile TAG species in a qualitative and semiquantitative manner. This method was called TriP-MS3 − triacylglycerol profiling using MS^3 − and provides unparalleled TAG coverage in a variety of matrices.

2. Material and methods

2.1. Chemicals and reagents

Internal standard (IS) d5-TAG 16:0/18:0/16:0 (cat# 860902), was purchased from Avanti Polar Lipids (Birmingham, AL). LC-MS-grade solvents and mobile phase modifiers were obtained from Fisher Scientific (water, methanol), Sigma−Aldrich (ammonium acetate, methyl-tert butyl ether (MTBE)) and Acros Organics (dichloromethane).

2.2. Human plasma

Lyophilized control plasma (Sciex, cat# 4386703) was reconstituted following vendor specifications. For linearity analysis, lyophilized control plasma was reconstituted at 10X (10 times concentrated relative to normal plasma concentration) and serial dilutions were performed until 0.01X (100 times diluted).

2.3. HepG2 cells and culture condition

Human hepatocellular blastoma cells (HepG2) (ATCC HB8065) were cultured in Gibco Dulbecco's Modified Eagle Medium:-Nutrient Mixture F-12 (DMEM/F-12, 1:1) (Thermo Fisher Scientific, cat# 11320033) supplemented with 10% fetal bovine serum and 1% penicillin/streptomycin, and maintained in an incubator at 37 °C under humidified 5% CO_2 conditions. A stock solution of the Δ5/Δ6 desaturase inhibitor CP-24879 (Sigma Aldrich, cat# C9115), was prepared at 30 mM concentration in DMSO. HepG2 cells were seeded in 100 mm tissue-culture treated dishes (40,000 cells cm^{-2}) and treated 72 h after seeding with 0.1% DMSO (control) or 30 μM CP-24879 in complete DMEM/F-12. After 24 h, cells were rinsed with warm Dulbecco's phosphate buffered saline (DPBS), trypsinized, resuspended in 2 mL DPBS after centrifugation (500 g for 5 min) and counted (Bio-Rad TC20 automated cell counter). Cell suspensions were centrifuged at 500 g for 10 min at 4 °C, supernatants were discarded, and cell pellets were stored at −80 °C until extraction for MS analysis.

2.4. Caenorhabditis elegans lipid droplets

Lipid droplet isolation was performed from whole worms as described before with small alterations [20]. Briefly, 2000 synchronized adult day 1 hermaphrodite *C. elegans* were used for a 2 h egg lay on 10 large 10 cm RNAi plates. After 72 h, worms were washed off the plates, collected by gravity settling and washed one time with PBS. Worms were transferred to empty RNAi plates for 15 min to clear bacteria from the gut. Worms were transferred in 25 mM Tris−HCl; 1 mM EDTA and protease inhibitor cocktail (Sigma Aldrich, P2714) and lysed with 7 strokes in a pre-chilled wheat stainless-steel tissue grinder. From here on all steps were performed on ice and solutions were precooled. Lysate was centrifuged at 4 °C at 200 g for 5 min. An equal volume of sucrose was added and centrifuged at 4 °C at 200 g for 5 min. Supernatant was transferred to a 13.2 mL thin wall ultraclear centrifuge tube (Beckman-Coulter) and layered with a gradient of 0.27 M sucrose, 0.135 M sucrose and 750 μL top solution buffer (25 mM Tris−HCl; 1 mM EDTA; protease inhibitor (Sigma Aldrich, P2714)). The samples were centrifuged in a SW41 Ti swinging bucket rotor using a Beckman XE-90 ultracentrifuge at 35,000 rpm for 30 min at 4 °C. The top cloudy layer which contained the lipid droplets was transferred via a glass pipet to a protein low bind Eppendorf tube and spun at 18,000 g for 10 min. The bottom, aqueous layer was removed, approximately 500 μL of supernatant was shock frozen in

liquid nitrogen and stored at −80 °C until extraction for MS analysis. Purity of the lipid droplet isolation was measured by Western blot.

2.5. Lipid extraction

Lipids were extracted in a random order using a biphasic separation with MTBE, methanol and water [21]. Briefly, 260 μL of ice-cold methanol and 40 μL of 0.01 mg mL^{-1} of d5-TAG IS in methanol:dichloromethane were added to 40 μL of sample (plasma or 4e6 − 6e6 HepG2 cells resuspended in 40 μL of water). The mixture was vortexed for 20 s and 1000 μL of ice-cold MTBE was added. Then the mixture was incubated under agitation for 30 min at 4 °C. After addition of 250 μL of water, the samples were vortexed for 1 min and centrifuged at 14,000 *g* for 10 min at room temperature. The upper phase containing the lipids was collected and dried down under nitrogen. The dry extracts were reconstituted with 300 μL of 9:1 methanol:toluene with 10 mM of ammonium acetate and centrifuged at 14,000 *g* for 5 min before analysis by MS. Water (40 μL) extracted using the same protocol was used as a blank control. For lipid droplets (~500 μL), the same protocol was used adjusting volumes to maintain the aqueous/organic solvents proportions.

2.6. TriP-MS3 method

2.6.1. Mass spectrometry

Flow injection analysis (FIA) was performed using 1:1 dichloromethane:methanol with 10 mM of ammonium acetate as running solution at 4 μL min^{-1} using a Nexera X2 UHPLC system (Shimadzu) and TAGs were analyzed using a QTRAP 5500 mass spectrometer (Sciex). The method comprises the following steps: 1) sample injection (50 μL, 0.75 min), 2) signal stabilization (3 min), 3) MS^3 followed by MRM data acquisition (14 and 5 min, respectively), 4) sample injection (50 μL, 0.75 min), 5) signal stabilization (3 min), 6) MS^3 data acquisition (14 min), and 7) system washing with running solution at 150 μL min^{-1} (4.5 min). The overall run time was 45 min per sample. Two injections were needed to acquire MS^3 data due to the time needed for the instrument to perform all the scans. The flow rate and injection volume were optimized so the signal was stable throughout the MS^3 and MRM acquisition time. In the protocol presented, MS^3 is run before MRM in the first injection but the order does not affect the method. MS parameters were set as follows: Spray Voltage = 4.1 kV (ESI positive mode), Temp. = 300 °C, Curtain gas = 17, Collision Gas = HIGH, Ion Source Gas 1 = 15, Ion Source Gas 2 = 32, Declustering Potential = 80, Entrance Potential = 10, Collision Energy = 36, Excitation Energy = 0.3. Collision energy for MRM and excitation energy for MS^3 experiments were optimized to yield the highest amount of neutral-loss ions in MRM mode and acyl cation ions in MS^3 modes using some of the most abundant TAGs in human plasma. These settings were then used for all the lipids detected with the method. TAG species were detected in positive mode with an ammonium adduct. The MS^3 and MRM transition lists are provided in Supplementary Tables 2 and 3, respectively. Data acquisition was performed in a random order.

2.6.2. Data processing

MRM transitions data and MS^3 spectra were quantified using MultiQuant (Sciex) and result tables were exported as text files. Downstream data processing was done using an in-house analysis pipeline written in R (version 3.6.2). Briefly, MRM signals lower than 5X blank signal were discarded and TAG features concentrations were estimated using the transition corresponding to the loss of FA 16:0 for the IS d5-TAG 16:0/18:0/16:0 by dividing endogenous TAG feature signal by IS signal and multiplying by IS concentration. The details explaining why this transition was used can be found in section 3.1. TAG species identification was performed at MS^3 level with the detection of both $[RCO]^+$ and $[MAG\text{-}H2O]^+$ ions from one or both of the two remaining fatty acids (the first one was lost during the MRM event). Peaks below a noise threshold were discarded with a threshold assigned to each MS^3 spectrum that was found to be proportional to MS^3 TIC. Threshold values may be dependent on the type of instrument and the status of the instrument. If no MS^3 peak was above the noise threshold for a given MRM transition, then the molecule was reported as a TAG feature. TAG species semiquantification was performed by summing signals from both $[RCO]^+$ and $[MAG\text{-}H2O]^+$ ions originating from the same FA. Then, signal intensities for each FA were normalized (ranging from 0 to 1) by dividing by the sum of all FA intensities detected in the MS^3 spectrum. Finally, TAG species concentration was determined by multiplying the normalized intensity to the concentration calculated at the MRM level. In cases where both FAs from the same TAG species were detected, both normalized intensities were summed before calculating the concentration. If a TAG species was measured in more than one MRM transition, the TAG species with the lower concentration was selected to prevent for overestimation in cases where a FA was present more than once in the molecule. Only the measurements of MRM transitions that do not correspond to pairs of TAG-FAs present in TAG species identified, are reported as TAG features. The calculations described above assume similar fragmentation and ionization efficiencies.

TAG species and TAG features with a coefficient of variation (CV) > 0.3 in biological triplicates (same sample, different extractions) were discarded (typically corresponding to less than 5% of the measurements). Absolute lipid concentrations were reported in plasma and HepG2 cells in μg mL^{-1} and μg.1e6 $cells^{-1}$, respectively. Relative abundances were reported for lipid droplets, where individual TAG abundances were normalized to total TAG.

2.7. LC-MS analysis

2.7.1. LC conditions

Lipids were separated using an Accucore C30 column 2.1 × 150 mm, 2.6 μm (Thermo Scientific, cat# 27826−152130) and mobile phase solvents consisted in 10 mM ammonium acetate and 0.1% formic acid in 60/40 acetonitrile/water (A) and 10 mM ammonium acetate and 0.1% formic acid in 90/10 isopropanol/acetonitrile (B). The gradient profile used was 30% B for 3 min, 30−43% B over 5 min, 43−50% B over 1 min, 55−90% B over 9 min, 90−99% B over 9 min and 99% B for 5 min. Lipids were eluted from the column at 0.2 mL min^{-1}, the oven temperature was set at 30 °C, and the injection volume was 5 μL. Autosampler temperature was set at 15 °C to prevent lipid aggregation.

2.7.2. Mass spectrometry

The Q Exactive plus was equipped with a HESI-II probe and operated in full MS scan mode for all the samples in positive mode. MS/MS spectra were acquired in data-dependent acquisition mode on pooled samples. The source conditions were as follows: Spray Voltage = 3.5 kV (ESI positive mode), Vaporizer = 200 °C, Capillary Temp. = 375 °C, S-Lens = 55.0%, Sheath Gas = 40, Auxiliary gas = 8, Sweep Gas = 0. The acquisition settings were as follows: AGC (MS) = 3e6, AGC (MS^2) = 1e5, Maximum Injection Time (MS) = 200 ms, Maximum Injection Time (MS^2) = 50 ms, Mass Range = 260−1900 Da, Resolution MS = 70,000 (FWHM at *m/z* 200), Resolution MS^2 = 35,000 (FWHM at *m/z* 200), MS^2 spectra were acquired in top-10 ions in each cycle, Isolation Window = 1.0 *m/z*, Dynamic Exclusion = 12 s, Normalized Collision Energy (NCE) = 25−30. External calibration was performed using an infusion of Pierce LTQ Velos ESI Positive Ion Calibration Solution.

2.7.3. Data processing

TAG species were identified by matching the precursor ion mass to a database and the experimental MS/MS spectra to a spectral library containing theoretical fragmentation spectra using LipidSearch software version 4.1 (Thermo Scientific) [22]. TAG species quantification was done using the IS d5-TAG 16:0/18:0/16:0. Peak areas of endogenous TAGs were divided by the IS peak area and multiplied by the IS concentration.

2.8. Statistical analysis

Technical triplicates (injections from the same sample) were used to calculate linearity and CV in section 3.2. Biological triplicates (measurements taken from distinct samples) were used in sections 3.3 and 3.5. To compare quantitative measurements using different methods, Pearson coefficient of determinations were calculated using mean log2 TAG species concentrations measured by TriP-MS3 and LC-MS methods. When analyzing TAG profile changes following treatment with a desaturase inhibitor in HepG2 cells, two-tailed Mann-Whitney test was performed on six biological replicates (measurements taken from distinct samples) and the p-values were adjusted for multiple comparisons using Benjamini–Hochberg method. As indicated in the figure captions, comparative analyses were performed at TAG group or FA composition levels. TAG group abundances were calculated by summing the concentration of all TAG species and TAG features containing the same number of carbons and unsaturations. FA composition was determined by summing the concentration of all TAG features and all TAG species containing a given FA. For TAG species with one FA present more than once, the concentration was multiplied by the number of times the FA was present in the molecule. The accuracy presented in Fig. S1 was calculated as follows: Error % = (|Calculated value-Reference value|)/Reference value × 100. The reference value corresponds to the concentration obtained with the LC-MS approach.

3. Results

3.1. TriP-MS3 method development

We sought to develop a MS method that would comprehensively quantify TAG species in any matrixes. In this context, we designed a hybrid method combining MRM and MS^3 experiments called TriP-MS3, leveraging the capabilities of quadrupole ion-trap instruments to perform both experiments on the fly. With this approach, the three FAs contained within each TAG molecule are identified as follows: 1) the identity of one FA is obtained from the MRM transition, 2) the daughter ion generated ($[M-(FA + NH3)]^+$) is collected in the ion-trap and further fragmented (MS^3) allowing the identification of a second FA as acyl cation ($[RCO]^+$) and/or $[MAG-H2O]^+$ ions (Fig. 1a), and 3) the identity of the third FA is deduced from the mass of the parent TAG species [12]. Hereafter, TAG molecules with known FA composition, including the number of carbons and unsaturations for each of the three FAs (*e.g.* TAG 16:0_16:1_18:0), will be referred to as "TAG species". FA (*sn*) and double bond positions are not considered. On the other hand, low abundance TAGs that do not meet the MS^3 sensitivity threshold (see section 2.6.2) are characterized by only one FA by MRM and are referred to as "TAG features" (*e.g.* TAG 50:1-FA 16:0).

The first step of the method development consisted in designing a transition list that would cover the maximum number of TAG species in a reasonable time frame. Typical MRM experiments for TAGs involves up to three transitions per TAG molecule; one for each FA. However, since MS^3 experiments contain information on the remaining two FAs, only one transition per molecule is needed which reduces the number of transitions. The MS^3 transition list was adapted from the Lipidyzer platform MRM transition list for TAGs [18]. This list was initially generated by selecting the minimum number of transitions to cover all possible TAG species composed of 40–62 carbons and containing at least one common FA with 14–22 carbons as listed in Supplementary Table 1. The criterion used to select transitions was to include FAs (*e.g.* 16:0, 16:1, 18:0 and 18:1) present in most FA combinations in each TAG group (*e.g.* TAG 50:1). As an example, only 4 TriP-MS3 transitions were necessary to cover 13 theoretical TAG species containing a total of 50 carbons and one unsaturation instead of 14 MRM transitions (Table 1). As a result, we obtained a time-effective MS^3 list containing 404 MRM transitions (Supplementary Table 2) that allows a semi-targeted screening of over 6,700 TAG species. Since MS^3 is less sensitive than MRM, low abundance TAG species that do not meet a certain intensity threshold are only measured in MRM mode and reported as TAG features with only one FA identified (see section 2.6.2). To increase the coverage in samples with low TAG concentration, 226 transitions from the Lipidyzer MRM list excluded in the MS^3 list were added to the MRM transition list expanding the final number of transitions to 630 (Supplementary Table 3). This strategy provides structural information for abundant species and high sensitivity detection for minor species.

TriP-MS3 was developed to estimate individual TAG species concentrations in an automated fashion. First, TAG feature abundances are estimated using one spiked-in deuterated TAG by dividing endogenous TAG feature signal by IS signal and multiplying by IS concentration. In this work, d5-TAG 16:0/18:0/16:0 is used and can be detected using two transitions corresponding to the neutral loss of FAs 16:0 and 18:0. The best transition was determined empirically by comparing the estimation accuracy with a LC-MS method. The highest accuracy was obtained using the transition corresponding to the loss of two FAs 16:0 (Supplementary Fig. 1). Second, the relative abundance of TAG species identified within each transition are estimated from MS^3 fragment intensities and combined with the semiquantitative measurement of the corresponding transition (TAG feature) from the MRM acquisition to estimate TAG species concentrations (see section 2.6.2 for more details). In the example presented in Fig. 1b, the MS^3 spectrum originated from the transition corresponding to the loss of FA 16:0 from TAG 50:1 led to the identification of 3 individual TAG species including TAG 16:0_16:0_18:1, TAG 16:0_16:1_18:0 and TAG 16:0_14:0_20:1. This TAG feature TAG50:1-FA16:0 was quantified at the MRM level using the spiked-in deuterated TAG and was estimated at 10 $\mu g\ mL^{-1}$. Individual TAG species concentrations were then estimated by 1) calculating the proportion of each TAG species (ranging from 0 to 1) from the MS^3 spectrum (the signal from each FA belonging to the same TAG species were summed) and 2) multiplying by the TAG feature estimated concentration (see section 2.6.2 for more details). In this example, TAG 16:0_16:0_18:1, TAG 16:0_16:1_18:0 and TAG 16:0_14:0_20:1 estimated concentrations were 6 $\mu g\ mL^{-1}$, 3 $\mu g\ mL^{-1}$, and 1 $\mu g\ mL^{-1}$, respectively. Finally, a processing pipeline was developed to automatically report semiquantitative results from all detected TAG species and features (see section 2.6.2).

3.2. Technical performances of TriP-MS3

The performance of the method was assessed by evaluating the coverage, linearity, and intra- and inter-day reproducibility. TriP-MS3 identified 285 TAG species and 289 TAG features in human plasma demonstrating a high heterogeneity in composition and broad coverage (Fig. 2). To assess the linearity of the method, plasma samples were analyzed at different concentrations ranging 3 orders of magnitude from 10X (10 times concentrated) to 0.01X

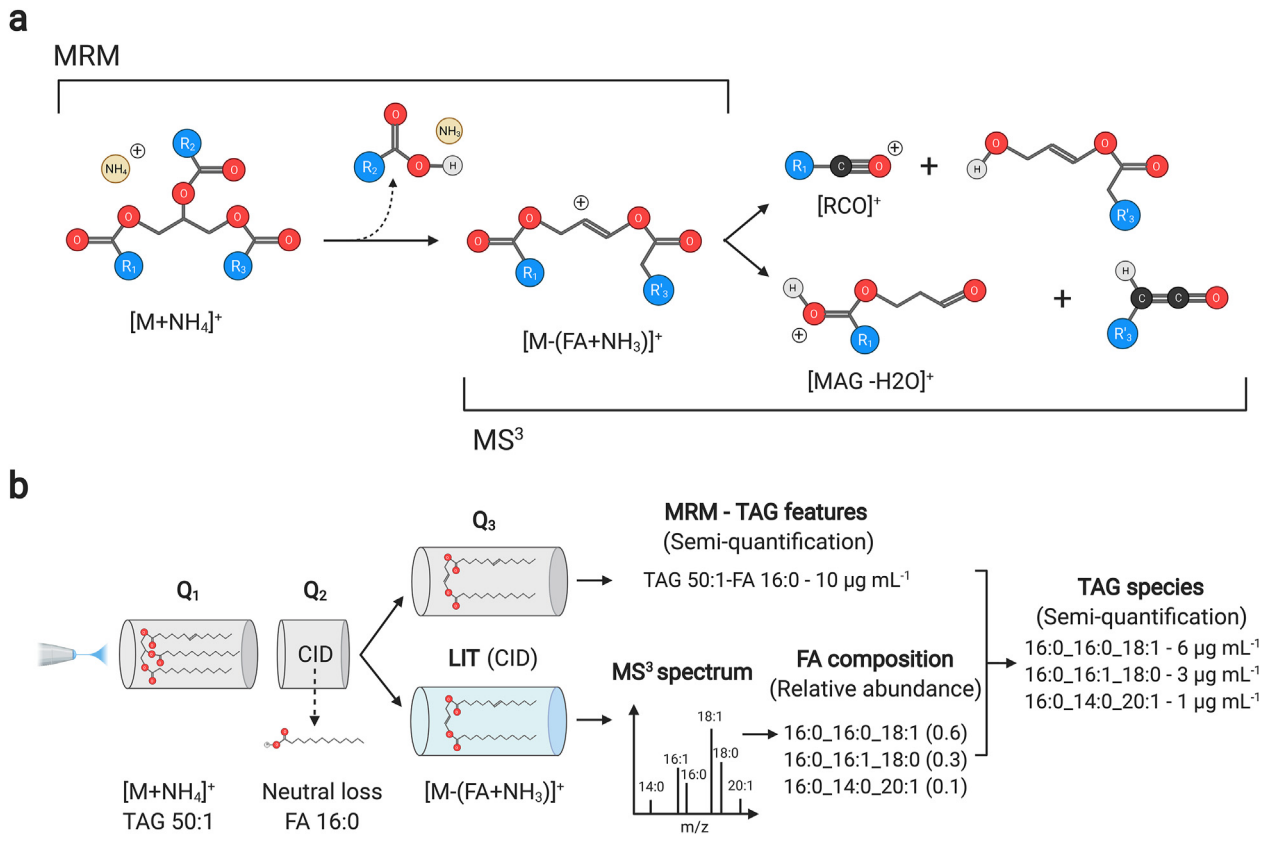

Fig. 1. Data acquisition principles of TriP-MS3. (a) Simplified schematic representation of species produced from MRM and MS^3 fragmentation experiments. MRM produces $[M-(FA + NH3)]^+$ following the neutral loss of one FA and MS^3 fragmentation of this ion generates up to 4 ions called $[RCO]^+$ and $[MAG-H2O]^+$ for each remaining 2 FAs. (b) TriP-MS3 identification and semiquantification workflow using TAG 50:1 as an example. Following the neutral loss of FA 16:0, the MS^3 spectrum present signal from 6 individual FAs leading to the identification of 3 individual TAG species TAG 16:0_16:0_18:1, TAG 16:0_16:1_18:0 and TAG 16:0_14:0_20:1. For simplicity, only the most abundant $[RCO]^+$ ions are represented for each FA. The TAG feature TAG 50:1-FA 16:0 concentration is estimated at the MRM level using the spiked-in deuterated TAG standard. TAG species concentrations are estimated using the relative abundance of signals from FAs at the MS^3 level.

Table 1
Number of transitions needed by MRM and TriP-MS3 approaches to cover 13 possible FA combinations in TAG 50:1. The first column contains 13 possible TAG species, the second column contains all the MRM transitions needed to measure all FAs present in those species. Finally, the third column contains the TriP-MS3 transitions necessary to measure all the 13 TAG species listed in the first column (there is no correlation in rows).

TAG 50:1 species (n = 13)	MRM transitions (n = 14)	TriP-MS3 transitions (n = 4)
14:0_16:0_20:1	TAG 50:1-FA 14:0	TAG 50:1-FA 16:0
14:0_16:1_20:0	TAG 50:1-FA 14:1	TAG 50:1-FA 16:1
14:1_16:0_20:0	TAG 50:1-FA 15:0	TAG 50:1-FA 18:0
14:0_18:0_18:1	TAG 50:1-FA 15:1	TAG 50:1-FA 18:1
14:1_18:0_18:0	TAG 50:1-FA 16:0	
15:0_17:0_18:1	TAG 50:1-FA 16:1	
15:1_17:0_18:0	TAG 50:1-FA 17:0	
15:0_17:1_18:0	TAG 50:1-FA 17:1	
15:0_16:0_19:1	TAG 50:1-FA 18:0	
15:1_16:0_19:0	TAG 50:1-FA 18:1	
15:0_16:1_19:0	TAG 50:1-FA 19:0	
16:0_16:1_18:0	TAG 50:1-FA 19:1	
16:0_16:0_18:1	TAG 50:1-FA 20:0	
	TAG 50:1-FA 20:1	

(100 times diluted) as compared to normal plasma concentration. At 0.01X, only 18 TAG species were fully characterized, however, 127 TAG features could still be measured. The number of TAG species increased substantially at higher concentrations with 240–293 species identified in samples ranging from 0.5X to 10X concentrated (Fig. 3a). The linearity of TAG species and TAG features was calculated on the whole range of concentrations (0.01-10X) but also on a restricted range that captures more TAG species (0.5-10X). The linearity was excellent for both ranges with all TAGs presenting a Pearson coefficient of determination (R^2) above 0.90 and a median R^2 above 0.97 (Fig. 3b). The dilution curve for TAG 18:1_18:0_16:0 is shown as an example in Fig. 3c. Intra- and inter-day reproducibility of Trip-MS3 was excellent with 93.8% and 91.4% of all TAG species and features detected in human plasma presenting a coefficient of variation (CV) < 0.2 (Fig. 3d).

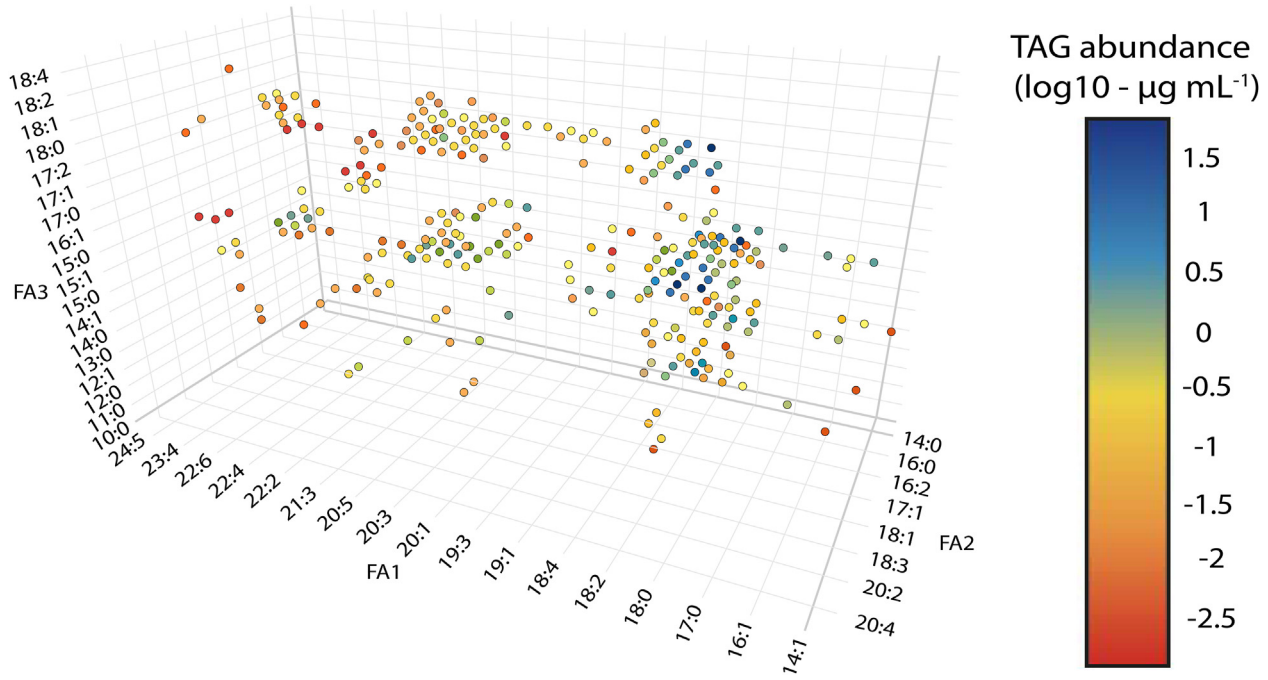

Fig. 2. Three-dimensional representation of individual TAG species identified in human plasma by TriP-MS3 (n = 285). Each dot is colored by its concentration and represents a TAG species composed of the FAs indicated on the axes.

3.3. Assessment of TriP-MS3 quantitative measurement accuracy

In order to validate the semiquantitative results obtained with TriP-MS3, we compared its performance with a RPLC-MS method using high chromatographic resolution (C30). We also compared the results with an MRM method using the MRM transition list of the Lipidyzer platform. In order to allow comparison of the three methods, TAG species and features concentrations were summed by number of carbons and unsaturations and the results were reported at the TAG group level (*e.g.* TAG 52:2).

Overall, the quantitative estimations obtained with Trip-MS3 approach were very similar to the LC-MS method (Fig. 4a). In addition, TAG species concentrations measured by Trip-MS3 and LC-MS methods correlated very well (R^2 = 0.834) demonstrating similar estimations at the species level (Fig. 4b). However, the MRM method overestimated the abundance of several TAG groups when compared to the LC-MS method. This overestimation was not equally distributed among all TAG groups and was more prominent for the most concentrated TAGs groups (*e.g.* TAG 50:1, TAG 50:2, TAG 52:2, and TAG 52:3) (Fig. 4a). This is explained by the fact that the same TAG species can be measured up to 3 times and the more abundant species are measured by more transitions compared to low abundant ones in the MRM transition list since it is optimized for human plasma. As shown in Table 1, TAG 16:1_18:0_16:0 can be measured as TAG 50:1-FA 16:0, TAG 50:1-FA 16:1, and TAG 50:1-FA 18:0. Moreover, in the MRM transition list of the Lipidyzer platform, the abundant TAG group 52:2 is measured by 9 transitions while the lower abundant TAG group 53:2 is measured with 4 transitions. In contrast, TriP-MS3 does not suffer from this problem since only one transition is used for each TAG species. Therefore, TriP-MS3 method circumvents this issue by only reporting non-redundant information.

3.4. TriP-MS3 suitability to recapitulate expected TAG composition changes in vitro

We determined whether our method could measure TAG profile changes following the treatment of a human liver cancer cell line (HepG2) with the Δ5/Δ6 desaturase inhibitor CP-24879 [23]. This cell line was selected due to the central role of hepatocytes in TAG metabolism [24]. In HepG2 cells, Trip-MS3 was able to quantify 350 TAG species and 228 TAG features. Inhibition of the desaturase activity is expected to result in an increase of TAGs containing saturated fatty acids (SFAs) and mono-unsaturated fatty acids (MUFAs) and a decrease of TAGs containing poly-unsaturated fatty acids (PUFAs) similarly to a recent report in mouse Inner Medullary Collecting Duct 3 (IMCD3) cells [25]. As expected, we observed an increase of TAGs containing SFAs and MUFAs at the FA composition and TAG group levels upon treatment with CP-24879 (Fig. 5). Semiquantitative estimates for all detected TAGs are reported in Supplementary Table 4.

3.5. Expanded coverage and versatility of TriP-MS3

The MRM transition list from the Lipidyzer platform was assembled with the objective to optimize coverage of lipids in blood. Hence, such a method will miss lipids with different FA composition in different biological samples (*e.g.* different organisms, cell types, tissues, biofluids, etc). In order to demonstrate the versatility of our TriP-MS3, the TAG content of human plasma and *C. elegans* lipid droplets as measured by MRM and TriP-MS3 were compared. *C. elegans* was selected as a proof-of-principle because of its unique TAG content; in particular TAGs in *C. elegans* are rich in FAs with odd carbon numbers [26]. TriP-MS3 successfully quantified 320 TAG species and 261 TAG features in *C. elegans* lipid droplets. In human plasma, the coverage of MRM and TriP-MS3 approaches was similar for the most abundant TAGs. However, TriP-MS3 expanded the coverage of less abundant TAGs including those with unconventional FAs species (*e.g.* 15:1, 17:1, 19:0, etc.) (Fig. 6a). In *C. elegans*, TriP-MS3 detected TAGs containing FAs with odd carbon numbers (e.g. 17:1, 19:1 and 19:0) that were missed by the MRM method (Fig. 6b). Some of these species were present in high concentrations including TAGs containing FA17:1 that were among the most abundant species. These observations are in line with previous studies showing high abundance of FA17:1 in *C. elegans* TAGs [27,28].

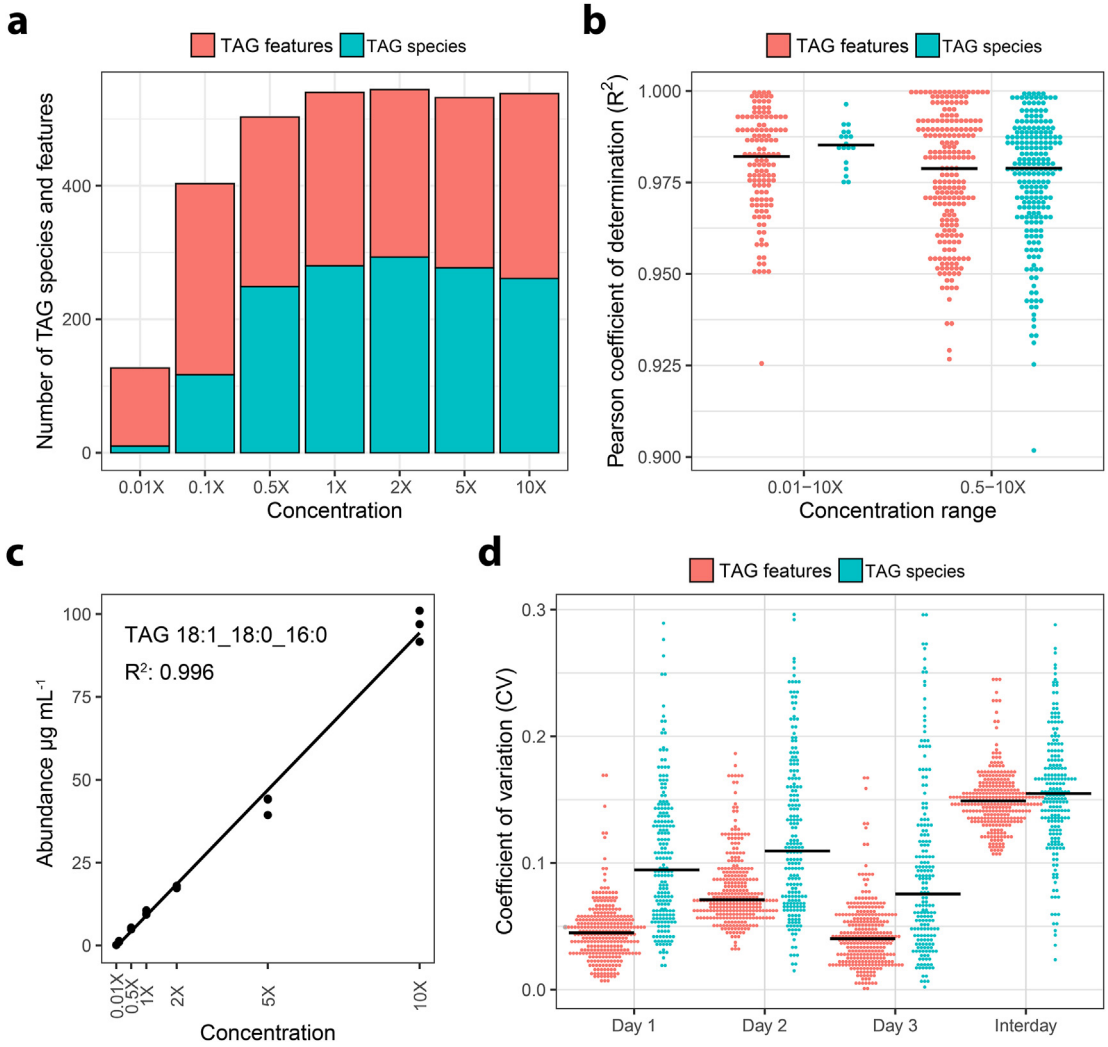

Fig. 3. Technical performances of TriP-MS3. (a) Number of TAG species and features identified at different human plasma concentrations. (b) TAG signal linearity reported with the Pearson coefficient of determination (R^2) calculated across two concentration ranges. The lower concentration range (0.01-10X) has 18 species and 127 features. The higher concentration range (0.5-10X) has 249 species and 254 features. (c) Dilution curve for TAG 18:1_18:0_16:0 across the whole range of concentrations. Each sample was analyzed in technical triplicates. (d) Intra- and inter-day variability was calculated on technical triplicates the same day and using the mean of each day, respectively. All TAG species (n = 285) and TAG features (n = 289) detected in 1X plasma were used in the analysis.

4. Discussion

In this work, we present a MS-based approach called TriP-MS3 for the comprehensive analysis of individual TAG species irrespective of the sample type. To the best of our knowledge, this is the first shotgun method designed to perform comprehensive individual TAG identification and semiquantification using a combination of MRM and MS^3 experiments. We demonstrated high coverage, sensitivity, linearity, and reproducibility as well as compared the concentration estimations with a state-of-the-art LC-MS method.

TriP-MS3 uses direct flow injection and thus circumvents many of the issues related to LC separation of TAG species. Even though column technologies have improved in the recent years with the introduction of high resolution C30 RPLC columns, base peak chromatographic separation of isobaric TAG species required to obtain accurate quantification remains challenging. In addition, retention time (RT) deviations often observed in large projects composed of hundreds of samples can impair RT alignment accuracy and thus quantitative measurements. Furthermore, annotation accuracy for LC-MS methods relies on the acquisition of high-quality MS/MS spectra ideally triggered at the apex of a peak. In reality, MS/MS experiments are often performed early or late in the peak increasing the chances of contaminating MS/MS spectra with fragments from isobaric TAGs eluting nearby which can lead to misidentifications [8,29].

In contrast to conventional targeted methods where each analyte needs to be previously considered before the acquisition, TriP-MS3 was designed to use the minimum number of MRM transitions and most possible fragment ions in MS^3 experiments are targeted to cover over 6,700 individual TAGs which provides increased coverage and versatility. TriP-MS3 was able to detect 285 TAG species in human plasma in comparison to state-of-the-art LC-MS methods with ~110 species [17] in the same time range (30 min−45 min total run time). We also demonstrate that TriP-MS3 was efficient in analyzing TAGs in different matrixes where TAG profiles vary substantially with the detection of 350 and 320 TAG species in human liver cells and C. *elegans*, respectively. For instance, Trip-MS3 successfully detected abundant TAGs containing odd chain FAs in *C. elegans* [27,28].

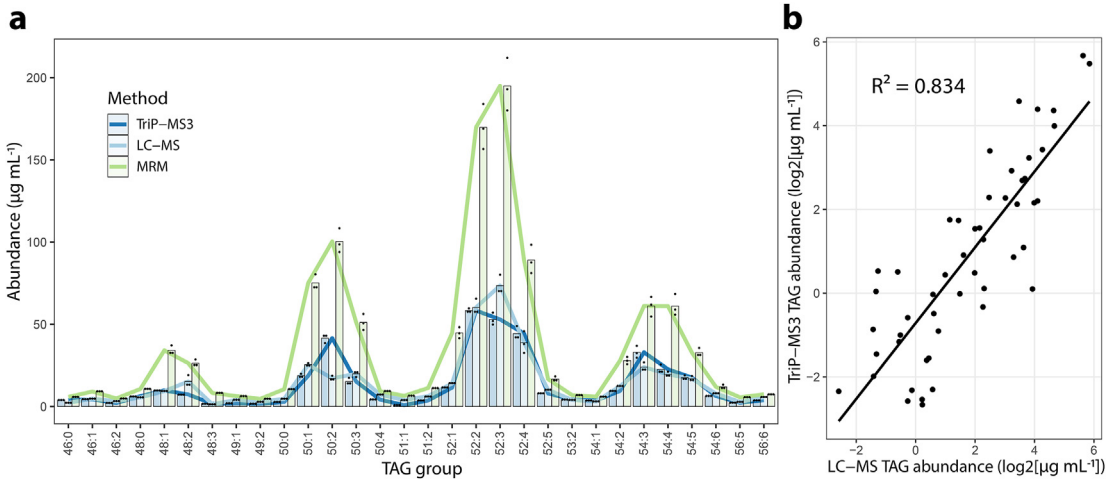

Fig. 4. Comparison of TriP-MS3 semiquantitative measurements with other methods. (a) Abundance of TAG groups in human plasma analyzed by three different approaches: TriP-MS3, LC-MS and MRM. TAG group abundances were calculated by summing the estimated concentrations of all TAG species and TAG features containing the same number of carbons and unsaturations. The bars represent the mean of biological triplicates (same sample prepared three times), the individual values are shown as dots. Lines connecting the mean measurement of each method were added to help compare the different approaches. (b) Correlation of semiquantitative measurements obtained with TriP-MS3 and LC-MS methods using the top 50 TAG species detected in human plasma. Average values from biological triplicates were used.

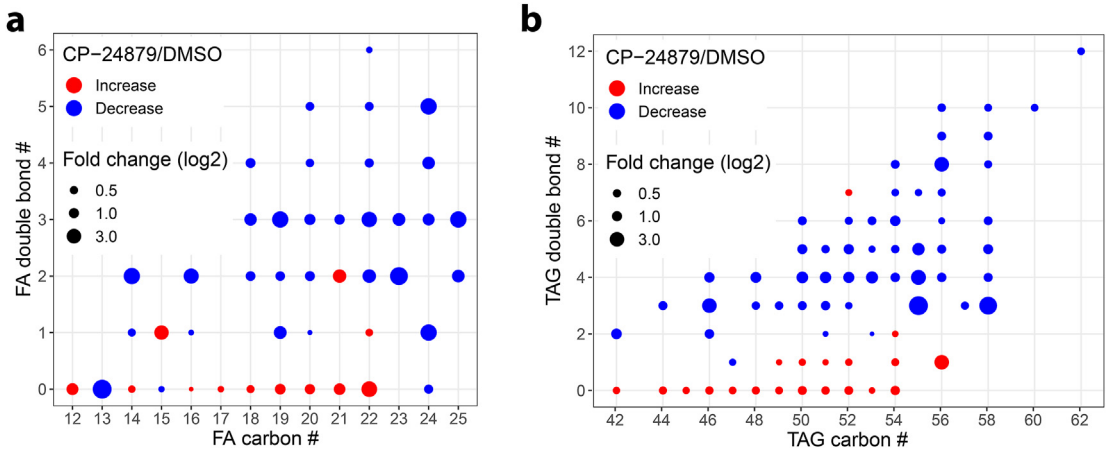

Fig. 5. TAG profile changes following treatment with a desaturase inhibitor. Changes at FA composition (a) and TAG group levels (b) in HepG2 cells treated with a Δ5/Δ6 desaturase inhibitor (CP-24879). The abundance of each TAG FA was calculated by summing the estimated concentration of all TAG features and all TAG species containing a given FA. For TAG species with one FA present more than once, the concentration was multiplied by the number of times the FA was present in the molecule. TAG group abundances were calculated by summing the estimated concentration of all TAG species and TAG features containing the same number of carbons and unsaturations. Species that increased or decreased with CP-24879 treatment were colored in red and blue, respectively. Biological sextuplicates were used in the analysis and only species with significant changes (Two-tailed Mann-Whitney, adjusted (Benjamini–Hochberg) p-value < 0.05) were shown. Fold changes of analytes detected in only one condition (infinite fold change) were plotted as fold change = 3.

Trip-MS3 is limited by the fact that it only reports the number of carbons and unsaturations in FAs; structural details such as linear or branched acyl chains, double bond, *sn*-positions, and cis/trans configurations are not distinguished. For instance, TriP-MS3 detects high levels of TAGs containing FA 17:1 in *C. elegans*, however, the FA measured is not a 17-carbon chain with one unsaturation but a dietary cyclopropane FA (FA 17Δ) [30]. In addition, Trip-MS3 doesn't differentiate fully esterified TAGs from TAGs with one or more alkyl-ether or alkenyl-ether fatty acids because of the instrument limited resolution. High resolution mass spectrometry (HRMS) is required to differentiate these species. In most cases, the impact will be minimal because ether-linked TAGs are typically present in very low abundance as reported previously [31,32].

Trip-MS3 provides semiquantification for a wide array of TAGs in a given sample. The accuracy of reported concentrations can be affected by differential fragmentation and ionization efficiencies as well as FA *sn*-position. In the presented method, we apply the same collision and excitation energies to all lipids which doesn't take into account varying fragmentation efficiencies depending on the TAG structure. In addition, the method doesn't consider FA (*sn*) positions which are known to impact the MRM fragmentation with FAs in sn-2 position being favored over FAs in sn-1 and sn-3 positions [12]. Despite these limitations, we have demonstrated that Trip-MS3 reports accurate TAG lipid species concentrations in comparison to a state-of-the-art RPLC-MS HRMS method using one IS.

To perform quantitative (instead of semiquantitative) analysis, each endogenous TAG should be quantified using a deuterated version of the same TAG. However, this option is impractical because i) one would need to know in advance which TAGs that will be detected in a sample, ii) a limited number of deuterated TAGs are commercially available and iii) the use of many IS will cause the experiment to be prohibitively expensive. Alternatively,

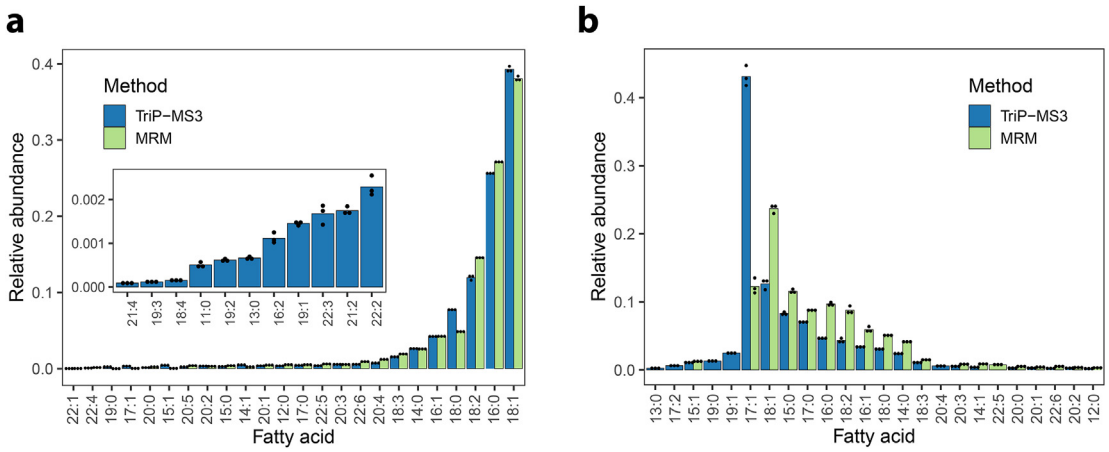

Fig. 6. Comparison of TAG coverage using the MRM and TriP-MS3 methods. Relative abundance of TAG FAs in human plasma (a) and in *C. elegans* lipid droplets (b). The abundance of each TAG FA was calculated by summing the estimated concentration of all TAG features and all TAG species containing the FA. For TAG species with one FA present more than once, the concentration was multiplied by the number of times the FA was present in the molecule. The concentrations were then normalized to the sum of all the species detected. The bars represent the mean of biological triplicates (same sample prepared in triplicates) and the individual values are shown as dots.

quantification could be performed using a handful of IS and selecting the most similar IS for quantification. However, such an approach will still be biased by the TAG FA composition [33]. For practicality, we decided to use one IS and estimate TAG species concentrations assuming similar ionization and fragmentation efficiencies IS [34]. A single IS is also typically used to quantify TAGs in LC-MS methods which suffer from the same biases [35]. However, direct infusion methods will produce more accurate results as compared to LC-MS approaches because of differential matrix interferences between the IS and the molecular species analyzed that elute at different retention times [33].

5. Conclusion

Altogether, TriP-MS3 combines the advantages of shotgun targeted methods (reproducible, sensitive, ease of data analysis) with a broader coverage and the level of structural information of untargeted LC-MS methods. We believe that the possibility to estimate in a high throughput manner not only TAGs concentrations but also their complete FA composition will be valuable to understand the role of these molecules in health and disease.

Data availability

The datasets generated and/or analyzed during the current study are available from the corresponding author on reasonable request. Kévin Contrepois, Department of Genetics, Stanford University, Stanford, California, USA. E-mail: kcontrep@stanford.edu.

Funding

This work was supported by grants from the National Institute of Health (NIH) 5RM1HG00773508, 1U2CCA233311-01 and 3U54HG010426-04S1. We also would like to acknowledge the support from Stanford Metabolic Health Center.

CRediT authorship contribution statement

Matias Cabruja: Conceptualization, Investigation, Methodology, Writing – original draft. **Josefina Priotti:** Investigation, Writing – review & editing. **Pablo Domizi:** Formal analysis. **Katharina Papsdorf:** Investigation. **Deanna L. Kroetz:** Supervision. **Anne Brunet:** Supervision. **Kévin Contrepois:** Conceptualization, Writing – review & editing, Supervision. **Michael P. Snyder:** Supervision, Funding acquisition.

Declaration of competing interest

The authors declare that they have no known competing financial interests or personal relationships that could have appeared to influence the work reported in this paper.

Acknowledgements

The authors would like to thank Mackenzie Pearson and Mathew Ellenberger for helpful technical discussions.

Appendix A. Supplementary data

Supplementary data to this article can be found online at https://doi.org/10.1016/j.aca.2021.339023.

References

[1] M. Ahmadian, R.E. Duncan, K. Jaworski, E. Sarkadi-Nagy, H.S. Sul, Triacylglycerol metabolism in adipose tissue, Future Lipidol. 2 (2) (2007 Apr) 229–237.
[2] A. Lass, R. Zimmermann, M. Oberer, R. Zechner, Lipolysis – a highly regulated multi-enzyme complex mediates the catabolism of cellular fat stores, Prog. Lipid Res. 50 (1) (2011 Jan 1) 14–27.
[3] R. Lehner, A.D. Quiroga, Chapter 5 - fatty acid handling in mammalian cells [Internet], in: N.D. Ridgway, R.S. McLeod (Eds.), Biochemistry of Lipids, Lipoproteins and Membranes, sixth ed., Elsevier, Boston, 2016 [cited 2021 Jan 5]. pp. 149–84. Available from: http://www.sciencedirect.com/science/article/pii/B9780444634382000055.
[4] E. Kassi, P. Pervanidou, G. Kaltsas, G. Chrousos, Metabolic syndrome: definitions and controversies, BMC Med. 9 (1) (2011 May 5) 48.
[5] E.P. Rhee, S. Cheng, M.G. Larson, G.A. Walford, G.D. Lewis, E. McCabe, et al., Lipid profiling identifies a triacylglycerol signature of insulin resistance and improves diabetes prediction in humans, J. Clin. Invest. 121 (4) (2011 Apr) 1402–1411.
[6] S. van Dieren, U. Nöthlings, Y.T. van der Schouw, A.M.W. Spijkerman, G.E.H.M. Rutten, A.D.L. van der, et al., Non-fasting lipids and risk of cardiovascular disease in patients with diabetes mellitus, Diabetologia 54 (1) (2011 Jan 1) 73–77.
[7] S.T. Ngo, F.J. Steyn, The interplay between metabolic homeostasis and neurodegeneration: insights into the neurometabolic nature of amyotrophic lateral sclerosis, Cell Regen. 4 (1) (2015 Aug 27) 5.
[8] F. Sanders, B. McNally, J.L. Griffin, Blood triacylglycerols: a lipidomic window on diet and disease, Biochem. Soc. Trans. 44 (2) (2016 Apr 15) 638–644.
[9] K. Contrepois, S. Wu, K.J. Moneghetti, D. Hornburg, S. Ahadi, M.-S. Tsai, et al., Molecular choreography of acute exercise, Cell 181 (5) (2020 May 28)

1112–1130, e16.
[10] S. Zarini, R.M. Barkley, M.A. Gijón, R.C. Murphy, Overview of lipid mass spectrometry and lipidomics, Methods Mol. Biol. Clifton NJ 1978 (2019) 81–105.
[11] R.C. Murphy, Challenges in mass spectrometry-based lipidomics of neutral lipids, TrAC Trends Anal. Chem. (Reference Ed.) 107 (2018 Oct 1) 91–98.
[12] A.M. McAnoy, C.C. Wu, R.C. Murphy, Direct qualitative analysis of triacylglycerols by electrospray mass spectrometry using a linear ion trap, J. Am. Soc. Mass Spectrom. 16 (9) (2005 Sep 1) 1498–1509.
[13] A.L. West, L.V. Michaelson, E.A. Miles, R.P. Haslam, K.A. Lillycrop, R. Georgescu, et al., Differential postprandial incorporation of 20:5n-3 and 22:6n-3 into individual plasma triacylglycerol and phosphatidylcholine molecular species in humans, Biochim Biophys. Acta BBA - Mol. Cell. Biol. Lipids. 1865 (8) (2020 Aug 1) 158710.
[14] K. Contrepois, S. Mahmoudi, B.K. Ubhi, K. Papsdorf, D. Hornburg, A. Brunet, et al., Cross-platform comparison of untargeted and targeted lipidomics approaches on aging mouse plasma, Sci. Rep. 8 (1) (2018 Dec 10) 17747.
[15] T. Cajka, O. Fiehn, LC–MS-Based lipidomics and automated identification of lipids using the LipidBlast in-silico MS/MS library [cited 2020 Jul 16], in: S.K. Bhattacharya (Ed.), Lipidomics: Methods and Protocols [Internet], Springer, New York, NY, 2017, pp. 149–170, https://doi.org/10.1007/978-1-4939-6996-8_14 (Methods in Molecular Biology). Available from:.
[16] Reiko Kiyonami, David Peake, Devin Drew, Xuefei Sun, Xiaodong Liu, Ken Miller, Large scale lipid profiling of a human serum lipidome using a high resolution accurate mass LC/MS/MS approach, ASMS (2015). Poster Note 64471.
[17] E. Rampler, A. Criscuolo, M. Zeller, Y. El Abiead, H. Schoeny, G. Hermann, et al., A novel lipidomics workflow for improved human plasma identification and quantification using RPLC-MSn methods and isotope dilution strategies, Anal. Chem. 90 (11) (2018 Jun 5) 6494–6501.
[18] Baljit Ubhi, Alex Conner, Steve Watkins, Eva Duchoslav, Annie Evans, Richard Robinson, et al. A novel lipid screening platform that provides a complete solution for lipidomics research. SCIEX Tech Appl. Note.
[19] R.C. Murphy, P.F. James, A.M. McAnoy, J. Krank, E. Duchoslav, R.M. Barkley, Detection of the abundance of diacylglycerol and triacylglycerol molecular species in cells using neutral loss mass spectrometry, Anal. Biochem. 366 (1) (2007 Jul 1) 59–70.
[20] H. Na, P. Zhang, Y. Chen, X. Zhu, Y. Liu, Y. Liu, et al., Identification of lipid droplet structure-like/resident proteins in Caenorhabditis elegans, Biochim Biophys. Acta BBA - Mol. Cell Res. 1853 (10) (2015 Oct 1). Part A):2481–91.
[21] V. Matyash, G. Liebisch, T.V. Kurzchalia, A. Shevchenko, D. Schwudke, Lipid extraction by methyl-tert-butyl ether for high-throughput lipidomics, J. Lipid Res. 49 (5) (2008 May) 1137–1146.
[22] R. Taguchi, M. Ishikawa, Precise and global identification of phospholipid molecular species by an Orbitrap mass spectrometer and automated search engine Lipid Search, J. Chromatogr. A 1217 (25) (2010 Jun 18) 4229–4239.
[23] M.G. Obukowicz, A. Raz, P.D. Pyla, J.G. Rico, J.M. Wendling, P. Needleman, Identification and characterization of a novel delta6/delta5 fatty acid desaturase inhibitor as a potential anti-inflammatory agent, Biochem. Pharmacol. 55 (7) (1998 Apr 1) 1045–1058.
[24] M. Alves-Bezerra, D.E. Cohen, Triglyceride metabolism in the liver, Comp. Physiol. 8 (1) (2017 Dec 12) 1–8.
[25] W. Kim, A. Deik, C. Gonzalez, M.E. Gonzalez, F. Fu, M. Ferrari, et al., Polyunsaturated fatty acid desaturation is a mechanism for glycolytic NAD+ recycling, Cell Metabol. 29 (4) (2019 02) 856–870, e7.
[26] P. Henry, O. Owopetu, D. Adisa, T. Nguyen, K. Anthony, D. Ijoni-Animadu, et al., Fatty acids composition of Caenorhabditis elegans using accurate mass GCMS-QTOF, J. Environ. Sci. Health Part B 51 (8) (2016 Aug 2) 546–552.
[27] D. Schwudke, J. Oegema, L. Burton, E. Entchev, J.T. Hannich, C.S. Ejsing, et al., Lipid profiling by multiple precursor and neutral loss scanning driven by the data-dependent acquisition, Anal. Chem. 78 (2) (2006 Jan 1) 585–595.
[28] J.K. Prasain, L. Wilson, H.D. Hoang, R. Moore, M.A. Miller, Comparative lipidomics of Caenorhabditis elegans metabolic disease models by SWATH non-targeted tandem mass spectrometry, Metabolites 5 (4) (2015 Nov 11) 677–696.
[29] A.P. Bowman, R.R. Abzalimov, A.A. Shvartsburg, Broad separation of isomeric lipids by high-resolution differential ion mobility spectrometry with tandem mass spectrometry, J. Am. Soc. Mass Spectrom. 28 (8) (2017 Aug 1) 1552–1561.
[30] J.L. Watts, M. Ristow, Lipid and carbohydrate metabolism in Caenorhabditis elegans, Genetics 207 (2) (2017 Oct 1) 413–446.
[31] S.R. Zanetti, M.I. Aveldaño, Long-term biopermanence of ceramides, cholesteryl esters, and ether-linked triglycerides with very-long-chain PUFA in the cadmium-damaged testis, Biochim Biophys. Acta BBA - Mol. Cell. Biol. Lipids. 1841 (1) (2014 Jan 1) 151–161.
[32] G.L. May, L.C. Wright, C.L. Lean, C.E. Mountfordt, Identification of 1-O-Alkyl-2,3-diacyl-sn-glycerol in plasma membranes of cancer cells, J. Magn. Reson. 1969 98 (3) (1992 Jul 1) 622–627.
[33] B. Burla, M. Arita, M. Arita, A.K. Bendt, A. Cazenave-Gassiot, E.A. Dennis, et al., MS-based lipidomics of human blood plasma: a community-initiated position paper to develop accepted guidelines, J. Lipid Res. 59 (10) (2018 Oct) 2001–2017.
[34] D. Schwudke, G. Liebisch, R. Herzog, G. Schmitz, A. Shevchenko, Shotgun lipidomics by tandem mass spectrometry under data-dependent acquisition control, in: Methods in Enzymology [Internet], Academic Press, 2007 [cited 2021 Mar 18]. pp. 175–91. (Lipidomics and Bioactive Lipids: Specialized Analytical Methods and Lipids in Disease; vol. 433). Available from: https://www.sciencedirect.com/science/article/pii/S0076687907330103.
[35] T. Cajka, J.T. Smilowitz, O. Fiehn, Validating quantitative untargeted lipidomics across nine liquid chromatography-high-resolution mass spectrometry platforms, Anal. Chem. 89 (22) (2017 Nov 21) 12360–12368.